



SPE/PS-CIM/CHOA 97905  
PS2005-97905

## Geomechanical Effects on the SAGD Process

Patrick M. Collins, PS-CIM/CHOA/SPE, Petroleum Geomechanics Inc.

Copyright 2005, SPE/PS-CIM/CHOA International Thermal Operations and Heavy Oil Symposium

This paper was prepared for presentation at the 2005 SPE International Thermal Operations and Heavy Oil Symposium held in Calgary, Alberta, Canada, 1–3 November 2005.

This paper was selected for presentation by an SPE/PS-CIM/CHOA Program Committee following review of information contained in a proposal submitted by the author. Contents of the paper, as presented, have not been reviewed by the Society of Petroleum Engineers, Petroleum Society-Canadian Institute of Mining, Metallurgy & Petroleum, or the Canadian Heavy Oil Association and are subject to correction by the author(s). The material, as presented, does not necessarily reflect any position of the SPE/PS-CIM/CHOA, its officers, or members. Papers presented at SPE and PS-CIM/CHOA meetings are subject to publication review by Editorial Committees of the SPE and PS-CIM/CHOA. Electronic reproduction, distribution, or storage of any part of this paper for commercial purposes without the written consent of the SPE or PS-CIM/CHOA is prohibited. Permission to reproduce in print is restricted to a proposal of not more than 300 words; illustrations may not be copied. The proposal must contain conspicuous acknowledgment of where and by whom the paper was presented. Write Librarian, SPE, P.O. Box 833836, Richardson, TX 75083-3836, U.S.A., fax 01-972-952-9435.

### Abstract

SAGD (steam-assisted gravity drainage) is a robust thermal process that has revolutionized the economic recovery of heavy oil and bitumen from the immense oil sands deposits in western Canada, which have 1.6 to 2.5 trillion barrels of oil in place. With steam injection, reservoir pressures and temperatures are raised. These elevated pressure and temperatures alter the rock stresses sufficiently to cause shear failure within and beyond the growing steam chamber. The associated increases in porosity, permeability, and water transmissibility accelerate the process. Pressures ahead of the steam chamber are substantially increased, which promote future growth of the steam chamber. A methodology for determining the optimum injection pressure for geomechanical enhancement is presented, which allows operators to custom-tailor steam pressures to their reservoirs.

In response, these geomechanical enhancements of porosity, permeability, and mobility alter the growth pattern of the steam chamber. The stresses in the rock will determine the directionality of the steam chamber growth, and these are largely a function of the reservoir depth and tectonic loading. By anticipating the SAGD growth pattern, operators can optimize on the orientation and spacing of their wells.

Monitoring of the SAGD process is central to understanding where the process has been successful. Methods of monitoring the steam chamber are presented, including the use of satellite radar interferometry. Monitoring is particularly important to ensure caprock integrity, as it is paramount that SAGD operations be contained within the reservoir.

There are several quarter-billion dollar SAGD projects in western Canada that are currently in the design stage. It is essential that these designs use a fuller understanding of the SAGD process in order to optimize on well placement and

facilities design. Only by including the interaction of SAGD and geomechanics can we achieve a more complete understanding of the process.

### Introduction

Geomechanics examines the engineering behaviour of rock formations under existing and imposed stress conditions. SAGD imposes elevated pressures and temperatures on the reservoir, which then has a geomechanical response. Typically, the SAGD process is used in unconsolidated sandstone reservoirs with very heavy oil or bitumen. In situ viscosities can exceed 5,000,000 mPa·s (mPa·s  $\equiv$  cP) under reservoir conditions.

These bituminous unconsolidated sandstones, or “oilsands” are unique engineering materials for two reasons: firstly, the bitumen is essentially a solid under virgin conditions; and secondly, the sands themselves are not loosely packed beach sands. Instead, they have a dense, interlocked structure that developed as a result of deeper burial and elevated temperatures over geological time. In western Canada, the silica pressure dissolution and re-deposition over 120 million years developed numerous concavo-convex grain contacts<sup>1,2</sup>, in response to the additional rock overburden and elevated temperatures. As such, these oilsands are at a density far in excess of that expected under current or previous overburden stresses. Furthermore, once oilsands are disturbed, the grain rotations and dislocations preclude any return to their undisturbed state.

Oilsands, by definition, have little to no cementation. As such, their strength is entirely dependent upon grain-to-grain contacts, which are considerable in their undisturbed state. These contacts are maintained by the effective confining stress. Any reduction in the effective confining stress will result in a reduction in strength. Since the SAGD process increases the formation fluid pressure, it reduces the effective stresses and weakens the oilsand.

**Disturbance.** Once the individual sand grains rotate and translate, there is an increase in bulk volume (“dilation”) due to an increase in porosity. The associated increase in absolute permeability can be a factor of 10. It is this remarkable behaviour of oilsand that makes geomechanics so important to the SAGD process.

**Figure 1** is a plot of normalized absolute permeability,  $k_a/(k_a)_{init}$ , versus volumetric strain (dilation) for triaxial tests on Athabasca oilsands. These specimens were cored vertically and horizontally from a block outcrop sample of

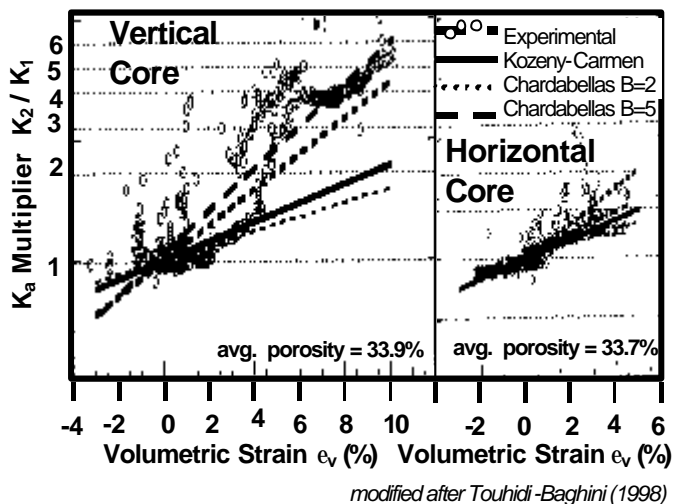


Figure 1 Absolute permeability increase during triaxial tests

non-bituminous oilsand from the McMurray Formation<sup>2,3</sup>. An isotropic confining stress was applied to each specimen, then an additional axial load was increased to failure. Volumetric strain and permeability were measured during the test.

Figure 1 shows the change in absolute permeability, with the normalized permeability serving as a permeability multiplier. As an example, the increase in vertical absolute permeability at a volumetric strain of 10% was a factor of 6. Increases for horizontal core are slightly less, as would be expected, given that the sand grains are slightly elongated and already provide a higher initial horizontal permeability. While some dilation occurs at stress levels below failure, dilation and its associated benefits are assured when the oilsands undergo shear failure.

Absolute permeability, as applied to oilsand, is an oxymoron: what is important is not what permeability exists, but what permeability is desired, and how much shearing is required to obtain it. Geomechanical enhancement of the absolute permeability is desirable, given that the SAGD production rate is proportional to the square root of permeability<sup>4</sup>; a magnitude of increase in permeability should increase the production rate by a factor of three.

From these tests, the virgin absolute permeabilities of clean Athabasca oilsand were determined to be  $k_v=1.0D$ ,  $k_h=1.5D$ . However, conventional physico-chemical laboratory tests typically provide values in excess of 10D. The cause for this discrepancy is core disturbance.

### Core Disturbance

Most disturbance occurs while coring. As the core is cut, it enters the PVC core liner (core tube) within the core barrel. The liner's internal diameter is typically 0.25 in. (~6mm) larger than the nominal core diameter in order to minimize frictional resistance as the core enters the liner.

The core fluid is undersaturated under virgin conditions, but becomes oversaturated at surface due to the drop in pressure. As a result, the solution gas exsolves as discrete bubbles within the bitumen. Since the bitumen is too viscous to displace or to allow gas to coalesce and escape, the bubbles expand within the pores. The unconsolidated structure of oilsand is unable to withstand this gas expansion. Therefore

the core expands to fill the core liner, permanently disrupting the grain-to-grain contacts.

**Conventional Methods.** This radial core expansion will result in about a 15% volumetric strain. This alone would result in an increase in  $k_a$  of an order of magnitude. In addition, once the core has expanded to fill the core tube, the gas has nowhere to escape and will expand in place, causing the core to expand longitudinally. In the field, core has been observed extruding itself from the core tube. Reported core recoveries in excess of 100% are indicative of this behaviour. Other evidence of core disturbance<sup>1</sup> includes:

- lateral and axial core expansion
- axial core extrusion from the inner core tube
- radial planes opening up within the core
- drilling-induced shear failure within the core
- drilling-induced cone-in-cone twist off within the core
- pervasive fracture networks in the mudstone portions
- drilling-induced core corrugation
- effervescing core, as gas continues to exsolve

Using a perforated core tube will eliminate the axial expansion, but not the radial expansion. Recompression of the core is ineffective, as it can only recover up to 50% of the volumetric strains. Recompression cannot restore the original structure, even when attempted at higher stresses than *in situ*.

**Core Storage.** Once the core has been retrieved to surface, the ends are capped and the core is immediately frozen. Freezing the core solidifies the connate water. More importantly, freezing drops the bitumen's (p,T) conditions back to an undersaturated condition. For this reason, freezing the core as quickly as possible (e.g.: with dry ice), and keeping it as cold as possible during transport and storage is essential to prevent further gas exsolution and its inherent core disturbance.

**Specimen Preparation.** Typically, when the frozen core arrives at the core laboratory it has already expanded to completely fill the core tube. The tube is then sawed longitudinally to expose the slabbed core for photographing. Cutting the core tube removes any remaining confining stress on the core, and the exposed core surface is usually allowed to thaw, both of which reinitiate the process of gas exsolution.

**Specimen Plugging.** The slabbed core is typically plugged by forcing a sharpened tube into partially thawed core. The core plug is then piston-extruded into a soft metal sleeve. This combination of shearing, compaction, and extrusion further disturbs the core, yet it is this core that is tested for permeability and porosity. Alternatively, core plugs can be taken by nitrogen coring, but this is not often done because of the additional cost, and is technically unjustifiable if the core arrived with excessive volumetric strain.

**Geomechanical Methods.** Special coring techniques must be used to obtain quality core suitable for geomechanical testing. These techniques minimize core expansion.

**Wireline.** The best method for retrieving bituminous oilsand is a triple-tube wireline system. This allows for the rapid retrieval of very short (1m to 2m) core runs without tripping the drillstring. Because gas exsolution is a time-dependent phenomenon, this rapid retrieval and freezing of bituminous core precludes almost all of the gas exsolution.

However, for oilsands containing heavy oil in which gas exsolution is faster, rapid retrieval may worsen core disturbance. Other methods, such as very slow retrieval, pressure coring, or downhole freezing, may be more suitable for heavy oils. SAGD is not commonly applied to oilsands with heavy oil since non-thermal recovery methods, such as CHOPS, are more economical.

Core runs are necessarily short to prevent the binding of core as it enters the inner core tube, and to prevent the core from failing in compression under its self-weight, particularly once the barrel is at surface where it is drained of drilling mud.

**Coring** should be done with low-invasion coring techniques:

- no gauge cutters on the core
- extended core shoe
- face mud nozzles
- low mud flow rates to prevent hydraulic erosion
- mud particulates designed to bridge the pore throats
- core catchers designed for unconsolidated core
- “zero” clearance inner core tubes

By using no gauge cutters on the core, the intent is to expose the core once, and only once, to the invasion of mud filtrate into the core. For bituminous core, filtrate invasion is much less of a problem since the bitumen is largely immobile at reservoir conditions.

**“Zero” Clearance Core Tubes.** For geomechanical-quality core, the PVC inner core tube should have “zero” clearance, i.e. an inner diameter 0.06 inches (~1.5mm) greater than the core diameter. This severely restricts the lateral expansion of the core, which preserves the core’s structure.

The frozen geomechanical core arrives at the laboratory in these inner core tubes. Since these core tubes have “zero” clearance, the core itself has not expanded significantly and is strengthened by the constraint offered by the core tube.

The core is not removed from the tubes for photography or specimen sampling. This may require some negotiation with regulatory bodies who may require regular sampling. Standard core studies can be done afterwards, in addition to geomechanical tests.

**Freezing.** The core is kept frozen in cold laboratory storage at temperatures down to  $-40^{\circ}\text{C}$ . This is to prevent gas exsolution. Some non-geomechanical specialists have speculated that freezing the core damages it, due to the expansion of the water as it transforms to ice. However, there is very little connate water in the undisturbed core, and the thermal contraction of the oil phase largely offsets the expansion of the water. Certainly any damage is far less for frozen core than it would be if the core were left non-frozen.

**Specimen Preparation.** The core is never allowed to thaw. Wearing winter gear, technicians prepare the core in a cold laboratory at  $-20^{\circ}\text{C}$  ( $-4^{\circ}\text{F}$ ). This is done to preclude or minimize gas exsolution. The core is removed from the core tubes and trimmed to specimen dimensions on a machine shop lathe. Ends are trimmed with a saw. During the specimen preparation, the specimen is periodically sealed and immersed in a cold bath (e.g.: liquid nitrogen) to keep the specimen in a deeply frozen state. Gas exsolution has been observed in specimens at  $-20^{\circ}\text{C}$ , therefore this precaution is necessary. The dimensioned specimen is mounted in the testing apparatus, and appropriate confining pressures are applied.

The specimen is then allowed to thaw. The indices of disturbance<sup>5,6</sup> for these specimens should be low, around 5%.

**Effective Permeability to Water.** The effect of shear dilation is more pronounced for cold, bitumen-rich oilsands. **Figure 2** shows the results of a series of triaxial tests on high quality bitumen-rich core<sup>7,8</sup>. The vertical axis is the effective permeability to water and the horizontal axis is the water saturation,  $S_w$ . The  $S_w$  increases as water is imbibed into the additional pore space created as these specimens dilated during testing. In these tests the bitumen was immobile: these tests were conducted at the reservoir temperature of  $8^{\circ}\text{C}$ , at which the bitumen viscosity was  $5 \times 10^6$  cP. The increase in water saturation is due solely to dilation and the creation of new pore space, which becomes occupied by water, and not by displacing the bitumen. This is not a relative permeability curve.

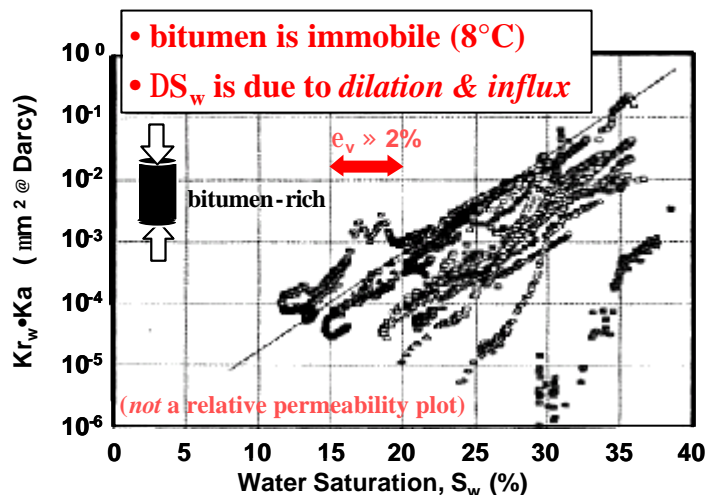


**Figure 2** Increased effective permeability to water during shearing of cold bitumen-rich oilsand  
mod. Chalaturmyk & Li (2001), after Oldakowski (1994)

The importance of this plot is that it shows the water permeability increased by three to four orders of magnitude. Even a small amount of dilation resulted in huge increases in water permeability. This has significant implications for pressure transmission into cold oilsands ahead of the steam chamber. (As reference, a 5% change in water saturation is approximately equal to a volumetric strain of 2%).

### Evidence of Shear Planes

**Laboratory.** When oilsand specimens are sheared, resulting in dilation, shear planes are evident throughout the specimens. **Figure 3** shows the results of triaxial tests<sup>9</sup> conducted on oilsands with a confining stress of 20 kPa. This figure shows a sequence of CAT scan slices through the core: light areas indicate lower density shear planes with higher porosity and higher permeability. Note the continuity of shear planes from one slice to another.

The importance of this is that shearing creates a dual porosity and dual permeability system that enhances the productivity of the formation. Shearing significantly enhances the SAGD process.

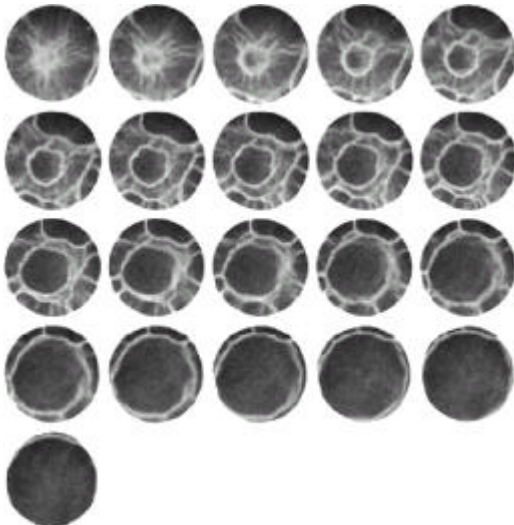


Figure 3 Shear bands in sheared Athabasca oil sand  
ref. Wong (2004)

**Field Evidence.** There is compelling field evidence that shearing occurs ahead of the steam chamber and that it has a beneficial effect. This is easily seen in the pressure and temperature behaviour observed in observation wells within the reservoir. **Figure 4** shows the temperature and pressure response over time for a stationary point ahead of the encroaching steam chamber<sup>10</sup>. The approach of the thermal front is regular and is indicative of conduction. The theoretical pressure front associated with that conductive thermal front is also shown. However, the actual pressure front arrives months beforehand, and the conclusion by the authors was that the pressure front was 8m to 12 m ahead of the temperature front. Note that the initial step-change in the pressure front cannot be pressure diffusion associated with the encroaching front since temperatures have not increased above the original reservoir temperature.

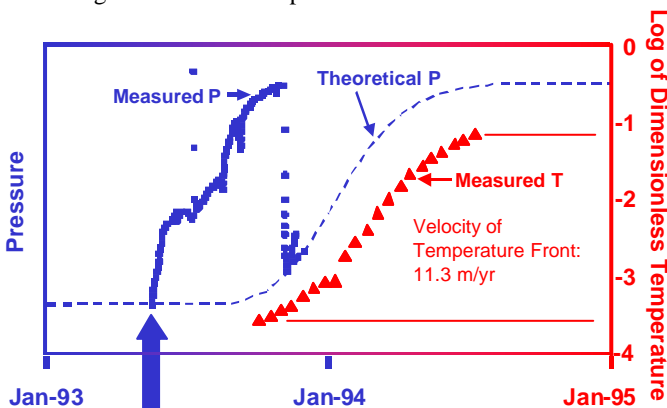


Figure 4 Transient (p,T) behaviour as the UTF Phase B steam chamber encroaches  
mod. Aherne & Birrell (2002)

An examination of the heat flux ahead of the SAGD steam chamber demonstrates that both conduction and convection contribute to the heat transfer to the cold formation. **Figure 5** shows the heat flux at a fixed point, with an encroaching steam chamber<sup>11</sup>. Conventional wisdom dictates that the only source of heat transfer to the cold formation ahead of the

steam chamber is conduction, yet during the early time convective heat transfer dominates. At temperatures below 50°C the bitumen is immobile. Furthermore, during the late time as the steam chamber encroaches, convection once again becomes very important

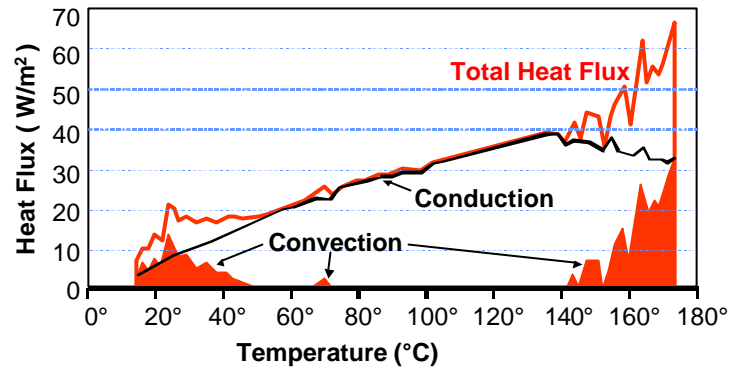


Figure 5 Convection and conduction ahead of a steam chamber  
ref. Birrell (2001)

This figure demonstrates that convection exists even when the bitumen is immobile. This spiky erratic convection curve shows that convective heat transfer consists of sporadic thermal intrusions. Convective heat transfer becomes a significant contribution to the total heat flux at temperatures exceeding 140°C, at which point the bitumen is very mobile. This behaviour is indicative of shear planes that are formed within the cold oilsand formation, thereby allowing hot fluids to enter these high porosity, high permeability conduits. These conduits become remobilized at temperatures above 140°C.

**Temperature Transients.** More compelling evidence for the existence of shear planes ahead of the steam chamber is provided by temperature data from a thermocouple string in the JACOS Hangingstone project<sup>12</sup>. **Figure 6** is a composite diagram: on the right is a schematic of the thermocouple (TC) string showing their locations relative to the horizontal injector and producer wells. The diagram on the left traces their temperature responses over time.

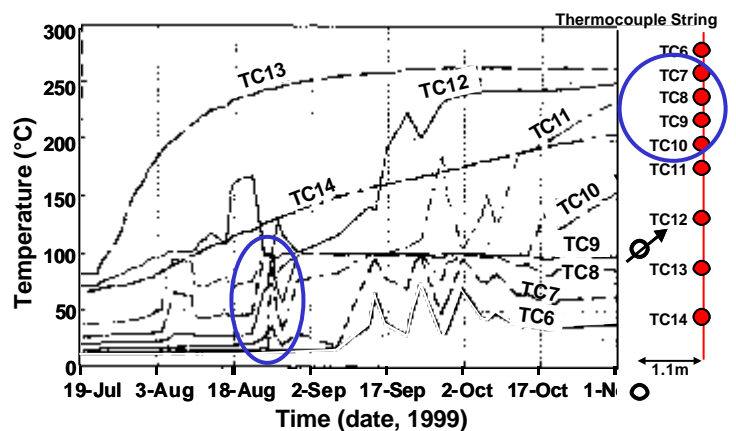


Figure 6 Temperature Changes in Observation Well OBB2 during the early period of SAGD process  
mod. Ito, Ichikawa, and Hirata (2000)



TC13 and TC14 are between the injector and producer wells and display a smooth, continuous increases in temperature over time. All other TCs are affected by thermal intrusions that are not conductive in origin. Hot fluids are entering the cold oilsands ahead of the steam chamber. As an example, the oval circles indicate a simultaneous event affecting four adjacent TCs. This indicates a vertical intrusion in a shear plane at or near the thermocouple string. Lastly TC6 and TC7 show repetitive interactions, which indicate that either an existing shear plane is being reactivated, or new plans are being created at each event. Note that these thermal signatures indicate spurt losses of hot fluids to the cold formation, many of which occur at temperatures far below that required for mobile bitumen. Furthermore, it is highly improbable that free gas is causing these thermal spikes because gas has insufficient thermal mass capacity to heat the rock to this extent. The only explanation is that hot water, with or without hot bitumen, has entered the formation through shear planes that are near-vertical in this project.

The compelling evidence for shearing within the oilsands formation and head of steam chamber is that:

- pressure increase is sudden and precedes the thermal front
- hot fluids are entering the cold oilsands beyond the steam chamber
- hot fluid intrusion is sporadic, sudden, temporal, and highly intrusive (~metres)
- flow paths either remobilize, or nearby paths are created

Shear planes are created with permanently enhanced porosity, permeability, and fluid mobility. The geomechanical behaviour ahead of the steam chamber can have a dominant beneficial effect on the SAGD process.

**Injection Pressures for Maximized Geomechanical Effects.**

While some beneficial effects can be obtained from shear displacements before failure, the maximum geomechanical benefits are obtained once the formation has failed in shear. The injection pressures at which rock formations will fail in shear can be calculated, knowing the existing rock stresses and pressures, and knowing the rock formation’s strengths.

**Rock Stresses.** The existing rock stresses are the primary driving force for shearing during SAGD. In reservoirs with high differential stresses, the rock is already part way to the failure envelope and will therefore require less injection pressure to cause the rock to fail. In western Canada, rock formations have high differential stresses due to the thrust regime of the Rocky Mountain orogeny: horizontal stresses perpendicular to the Rocky Mountains axis are very high and will exceed the vertical stress for shallower SAGD projects. **Figure 7** shows a typical profile of stress versus depth for oilsands in western Canada<sup>13</sup>. At shallow depths the vertical stress is the minimum principal stress, and it does not become the maximum principal stress except for the deepest projects.

A formation pressure profile is shown as a hydrostatic line. However, it is underpressured due to lateral draining through permeable formations that outcrop to river valleys<sup>14</sup>.

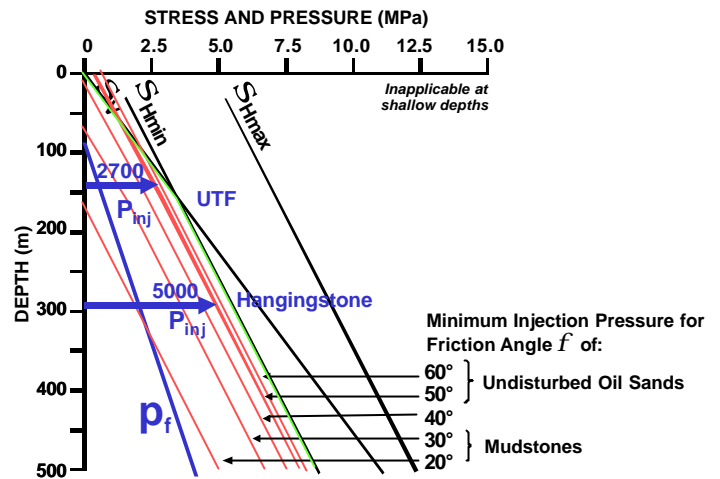


**Figure 7 Injection Pressures to Maximize Geomechanics**  
ref. Collins (2002)

Rock strengths for oilsands and their associated mudstones are well known<sup>15</sup>; strength data from disturbed specimens should not be used.

**Injection pressures.** Knowing the rock stresses, and the strength properties of the rock formations, the injection pressures that will result in shear failure can be calculated. This will maximize the geomechanical enhancement of the SAGD process. Typically, clean oilsand will have a friction angle of 50° to 60°; mudstones will have friction angles below 30°. **Figure 7** shows a series of injection pressure profiles required to induce shear failure, as a function of the rock’s friction angle. It is reasonable to use a friction angle of 50° for oilsands.

The injection pressures used in the original SAGD pilot, AOSTRA’s UTF Phase A project (now the Petro-Canada Dover project), were approximately 2700 kPa. At the projects relatively shallow depth of 140m to 162m, this was sufficient to induce shear failure of the oilsands. Similarly, the JACOS Hangingstone project injected at pressures of 5000 kPa, a pressure that was predetermined by conducting minifrac tests in order to quantify the rock stresses and ensure geomechanical enhancement of their SAGD process<sup>12</sup>.

**Rule-of-Thumb.** In general, to maximize geomechanical enhancement in western Canadian oilsands, the injection pressure should be:

$$P_{inj} \geq 15(\text{kPa/m}) \cdot z(\text{mTVD}) + 500\text{kPa} \dots\dots\dots [1]$$

where:

- \$P\_{inj}\$ is the injection pressure to achieve shear failure
- \$z\$ is the vertical depth (metres)

This will ensure that shear failure occurs within the oilsand, for any injection process. Expressed in another manner, \$P\_{inj}\$ should be within 500 kPa of the fracture pressure. While other geographic regions will have site-specific conditions, these are still likely to result in a \$P\_{inj}\$ close to the fracture pressure.

**High-Pressure versus Low-Pressure SAGD.** The optimal geomechanical injection pressure is higher than pressures currently being considered by many operators. Higher steam injection pressures require a higher steam:oil ratio (SOR). In the belief that a lower SOR is more economical, many operators are designing for lower injection pressures. However, this approach merely minimizes the amount of heat injected into the formation. A more logical approach would minimize the net energy, which must include the benefit of heat recovered from the produced fluids<sup>6</sup>. The recovered heat can reasonably be expected to be one half to two thirds of the heat injected. Since more heat is recovered at higher injection pressures, the conventional wisdom of the thermal benefits of operating at lower pressures is overstated.

Furthermore, our objective is neither to minimize the heat injected, nor to minimize the net energy injected, but to maximize the benefit to our companies without jeopardizing the resource. As such, the most rational approach is to maximize the net present value, which will vary with injection pressure. This evaluation must include both CAPEX and OPEX, which vary considerably with injection pressure.

Proponents of low pressure SAGD typically ignore all geomechanical effects and presume that permeability will be independent of injection pressure. Operators who forget the lesson of "pressure-enhanced vertical conformance"<sup>16</sup> may find that their effective permeabilities and SAGD performance are less than expected with low-pressure steam injection.

#### **Practical Operating Strategy: Ramped $P_{inj}$ .**

Injection pressures during wellpair start up should be high enough to shear the formation around the injector and producer wells. This will increase the wells' productivity indices by creating a negative skin, enhance interwell communication by creating a highly disturbed zone around the wellpairs, accelerate interwell heating by convective heat flux, and greatly increase the fluid mobility by increasing the water saturation within the newly-disturbed zone. The added benefit of reduced viscosities at the higher temperatures associated with higher steam pressures is a second-order effect.

As the steam chamber grows, the top of the steam chamber will dictate the current maximum operating pressure. In any given rock formation, the stresses are almost always lower at shallower depths and therefore the fracture pressure is also lower. Since the hydrostatic gradient of the steam column is far less than the fracture gradient, the operating pressure must be reduced as the chamber rises or the steam will fracture the formation. This reduction in the operating pressure may be significant for those relying on the steam pressure lifting the produced fluids to surface, particularly as the project matures and the steam reaches the caprock. This is especially a concern after periods of shut-in, at which time the hydrostatic column in the production tubing is filled with liquids that cannot flash. (Flashing of some produced water would unload the backpressure exerted by the fluid column.)

As the steam chamber rises, the injection pressure should be gradually reduced, but kept within 500 kPa of the fracture pressure. This will ensure that geomechanical shearing continues, yet allow a safety margin of over 20m as to the elevation of the top of the steam chamber. Once the top of the steam chamber rises to its final elevation, pressures can be

maintained constant until blowdown, at which time the operating pressures are reduced in order to recover some of the heat stored in the rock matrix. By this stage, the reservoir should be sufficiently sheared to ensure continued high performance. The drop in pressure will have little to no effect on the enhanced porosity and permeability since these changes are permanent and irreversible.

**Exception: Thief Zones.** An exception to the proposed operating strategy is when thief zones are in potential contact with the reservoir. Thief zones are high transmissibility zones that could allow the escape of reservoir fluids, or the inflow of water. Common examples are the presence of a gas or water cap above the chamber, or a basal water leg. Steam chamber breakthrough to a gas cap would require a steam pressure that would balance the gas cap pressure. This would minimize any loss of steam to the gas cap, and reduce the propensity of depleting the gas cap that could result in the encroachment of a water leg. Steam chamber contact with an overlying water leg would likely be disastrous, even if operating at balanced pressures, since the water leg would drain into the steam chamber and quench the process.

The pressure at the contact between the reservoir and any basal water leg must also be balanced, which should include any hydrostatic effects of the condensed water and hot bitumen below the steam chamber. Water inflow could quench the process, and the outflow of hot water is not only a severe energy loss, but it could mobilize a conduit through which hot bitumen would be lost. Bitumen plugging of a basal water leg is not assured, within economical limits, if the continuous heat loss by water convection maintains a temperature at which the bitumen remains mobile.

**Thief Zone Operating Strategy.** The objective is to minimize fluid exchange between the reservoir and the thief zone. Steam injection pressures should start high and be ramped down, as before, until breakthrough is imminent. Partial blowdown should proceed until pressures are matched between the reservoir and the thief zone at breakthrough. Balanced pressures should be maintained afterwards, which may preclude further blowdown at the end of the project.

#### **Effects of Shear Plane Orientation**

The effects of shearing will neither be uniform nor be the same for all reservoirs. Due to the directionality of the three principal stresses within any reservoir, the preferential direction of shearing will vary. However, in western Canada there are three broad classes of SAGD reservoir: shallow, mid-depth, and deep, as determined by the relative magnitudes of the vertical stress, minimum horizontal stress, and the maximum horizontal stress. These three classes are analogous to the stress regimes of thrust faulting, strike-slip faulting, and normal faulting.

**Shallow SAGD** is defined as projects where the vertical stress is the minimum *in situ* stress (e.g.: UTF/Dover, Mackay River, Firebag, Joslyn Creek). Once shearing is induced with an adequate injection pressure, the dominant orientation of shear planes will be  $\pm 15^\circ$  to  $20^\circ$  from the horizontal plane. These planes will be inclined in the direction of the maximum horizontal stress, which is oriented NE-SW in the oil sands of western Canada<sup>17</sup>.

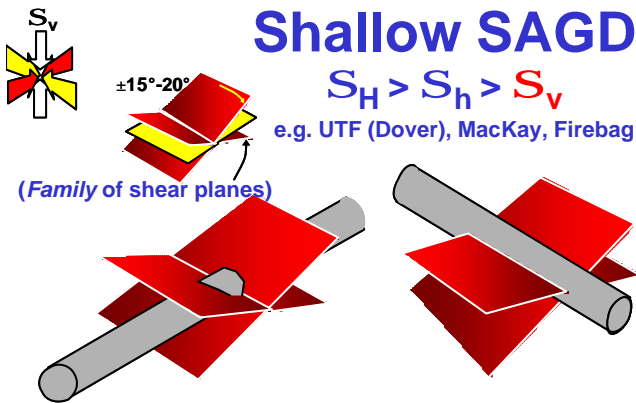


Figure 8 Shallow SAGD - induced shear plane orientations

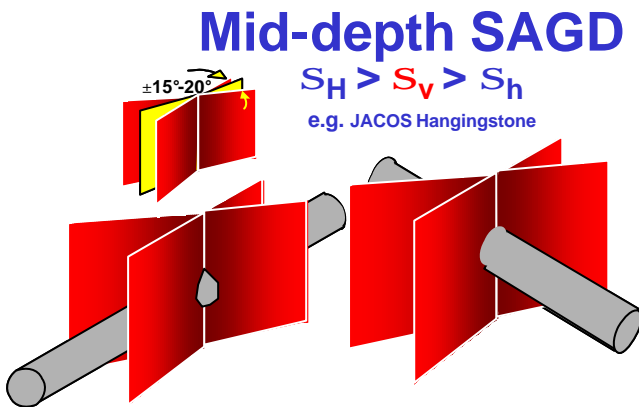


Figure 9 Mid-depth SAGD - induced shear plane orientations

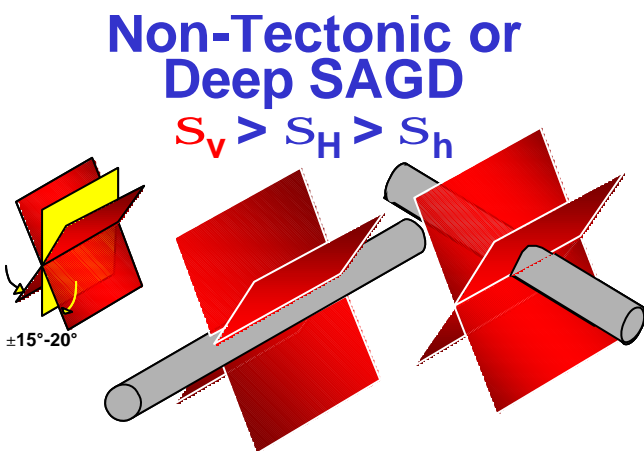


Figure 10 Deep SAGD - induced shear plane orientations

Multiple inclined shear planes will transect the horizontal wells, but a family of similar planes exist away from the wellpairs, and will be connected to them through a shear plane network. **Figure 8** idealizes these shear planes as pairs of rectangular conjugate planes forming an “X”. In reality, these will not necessarily be in pairs nor always intersect the wellbores. Their shape will be not likely be rectangular.

Two different cases are shown: horizontal wells drilled parallel and perpendicular to the maximum horizontal stress,  $\sigma_{Hmax}$ . (The direction of  $\sigma_{Hmax}$  is from the bottom-left to top-right in all three figures, parallel to the red arrows in the top left corner.)

**Wells Parallel to  $S_{Hmax}$ .** These shear planes will accelerate wellpair start-up since they will transect both the injector and producer wells. There will be a preferential longitudinal growth of the steam chamber, which will have a flat aspect ratio of height to width due to the low inclination of the shear planes.

**Wells Perpendicular to  $S_{Hmax}$ .** Start-up will be slightly slower because any single shear plane will not intersect both the injector and producer wells. Interwell communication will come from the network of shear planes. More significantly, there will be high lateral growth of the steam chamber, which should permit larger wellpair spacing. The steam chamber will also have a flat aspect ratio.

**Mid-Depth SAGD** projects have a vertical stress that is the intermediate principal stress (e.g.: Hangingstone). The dominant orientation of induced shear planes will be in the vertical plane, aligned  $\pm 15^\circ$  to  $20^\circ$  to the maximum horizontal stress orientation. Again, a family of planes will exist throughout the reservoir, and will be connected to the wellpairs through this network of shear planes. As in the previous case, **Figure 9** idealizes these shear planes as pairs of conjugate planes forming an “X”.

**Wells Parallel to  $S_{Hmax}$ .** These shear planes will result in a rapid wellpair start-up: the planes will transect both the injector and producer wells, with that communication being vertical. Vertical steam chamber growth will be rapid <sup>12</sup>, e.g.: 1m/day. There will be a preferential vertical and longitudinal growth of the steam chamber, which will have a high aspect ratio of height to width due to the vertical shear planes.

**Wells Perpendicular to  $S_{Hmax}$ .** Start-up will also be rapid, with these planes intersecting both the injector and producer wells. Vertical steam chamber growth will be rapid. Again, there will be high lateral growth of the steam chamber, which should permit larger wellpair spacing. The steam chamber will have a high aspect ratio.

**Deep SAGD** projects have a vertical stress that is the maximum principal stress (possibly Peace River). The dominant orientation of induced shear planes will be  $\pm 15^\circ$  to  $20^\circ$  to the vertical plane, aligned parallel to the maximum horizontal stress orientation, as idealized in **Figure 10**. Again, a family of planes will exist throughout the reservoir, and will be connected to the wellpairs through this network of shear planes.

**Wells Parallel to  $S_{Hmax}$ .** These shear planes will result in fairly rapid wellpair start-up, since the near-vertical planes

transecting the injector and producer wells will enhance vertical communication. Vertical steam chamber growth will also be rapid. There will be a preferential longitudinal and vertical growth of the steam chamber, which will have a high aspect ratio of height to width.

**Wells Perpendicular to  $\sigma_{Hmax}$ .** Start-up will be more rapid, since these planes intersect both the injector and producer wells. Vertical steam chamber growth will be rapid. There will also be high lateral growth of the steam chamber, which should permit larger wellpair spacing. The steam chamber may have a high aspect ratio if the vertical growth outpaces the lateral growth.

**Directional Bias.** There is an upward bias in the growth of shear planes. This is because stresses are lower at shallower depths; therefore it is easier for fractures or shear planes to grow upwards rather than downwards. As such, high-pressure injection into oilsand may result in a bowl-shaped network of shear planes and fractures<sup>18,19</sup>. Fortunately, the horizontal wellpairs are placed at the bottom of the reservoir therefore the preferential upward growth of shear planes is not an impediment to the SAGD process.

**Supplemental thermal effects.** Heating induces additional compressive stresses that are largest in the preferential direction of steam chamber growth. These stresses are transferred to the cold oilsands ahead of the steam chamber. This induces shearing ahead of the steam chamber that promotes steam chamber growth. As such, accelerated start-up should be expected for wells drilled in the direction of the  $\sigma_{Hmax}$  orientation. More importantly, enhanced inter-wellpair coalescence will occur for wells drilled perpendicular to the  $\sigma_{Hmax}$  orientation.

**Thermal Jacking.** The steam chamber will create a heated zone that will exert ever increasing outward compressive stresses. This thermally expanded heated zone will displace the caprock and overburden upwards (“thermal jacking”) which will increase the vertical stress over the wellpairs, and relieve some of the vertical stress between wellpairs<sup>15</sup>. This vertical stress relief ahead of the steam chamber will enhance steam chamber growth in shallow SAGD projects but be detrimental to deeper projects.

**Wellpair Interference.** Horizontal thermal compressive stresses around two or more wellpair will be additive once the stress fields of the wellpairs interfere. This will favour lateral growth for wells drilled perpendicular to the  $\sigma_{Hmax}$  orientation, and inhibit lateral growth for wells parallel to  $\sigma_{Hmax}$ .

**Effects on Well Performance.** Wells drilled parallel to the  $\sigma_{Hmax}$  orientation are aligned with induced shear planes, and will have a rapid start-up. Wells drilled perpendicular to this will intersect the induced shear planes, and will access the reservoir best in the long term. Given that fast start-up can always be achieved with a higher initial steam injection pressure, drilling the wells perpendicular to  $\sigma_{Hmax}$  will provide the most benefit.

### Theoretical vs. Actual Steam Chamber Growth.

Conventional wisdom has the steam chamber immediately rising to the top of the reservoir, and then spreading laterally as an inverted triangle. This continues until the steam chambers of adjacent wellpairs coalesce, at which time the sideslopes of the base of each triangle continue to flatten. This is what occurred in the laboratory, it occurs in most reservoir simulations, but it does not occur in practice.

The most completely documented growth of a SAGD steam chamber was that of the UTF Phase A “laboratory-scale” pilot. This pilot consisted of three wellpairs spaced 25m apart, and having 55m of completion length over the horizontal wells. There were 26 vertical observation wells installed within that nominal 55m × 7m pattern, equivalent to a well density of over 17,000 wells per section. The reservoir interval was shallow, between the depths of 140m and 162m. The top half of the 22m-thick pay zone was a clean oilsand, deposited as cross-trough beds. The bottom half was a massive, structureless clean channel sand. By an unfortunate happenstance, a 1.4m-thick massive mudstone was found to lie between the injector and producer wells after they were drilled. Otherwise, there were few mudstone stringers detected throughout the oilsand. Only above the reservoir did the deposit degrade into interbedded sands and mudstones.

A majority of observation wells were concentrated along the “geotechnical cross-section” which transected the three wellpairs. This provided an excellent means to measure the lateral growth of the steam chamber.

The steam chamber did not immediately rise to the top of the oilsands, or even to the top of the clean channel oilsands. Instead, the characteristic growth was lozenge-shaped (**Figure 11**), or as poetically described by Ito & Suzuki (1996)<sup>20</sup>:

*“The steam chamber grows upwards and outwards simultaneously like the expansion of dough during baking. This outward growth does not spread along the top of the reservoir.”*

This is the same growth pattern as predicted for a shallow SAGD project with geomechanical shearing of the oilsand.

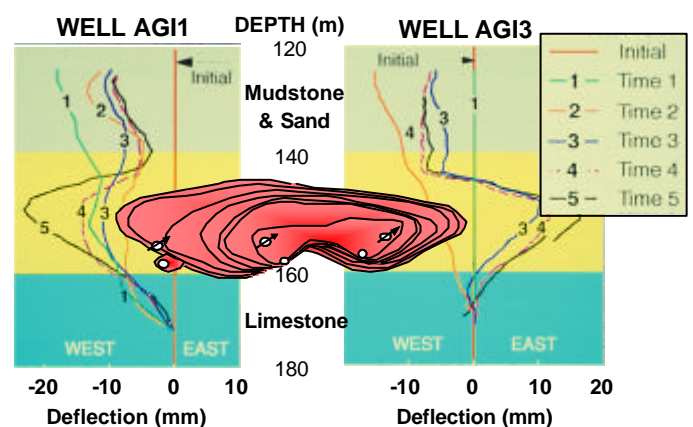


**Figure 11 Expansive lateral strains, UTF Phase A**  
ref Collins (1994); insert ref. Ito & Suzuki (1996)



### Reservoir Deformations.

The shearing and dilation of the oilsands results in a volume increase within the reservoir. This exerts outward displacements, away from the steam chamber. In the UTF Phase A pilot, lateral displacements were measured with precision gyrosurveys in cased inclinometer wells<sup>21</sup>. **Figure 11** shows the lateral displacements of two observation wells located on either side of the three-wellpair pattern. The schematic in the centre shows the expanding steam chamber at the geotechnical cross-section.

The displacement profiles show increases in outward displacement over time. The maximum lateral displacement occurs when the steam chamber is largest, and at the elevation where the steam chamber is widest. The shear deformations within the reservoir are real and would be larger for a commercial pattern.

**Vertical Strains** within the reservoir can also be measured with extensometers permanently installed in the oilsands. The UTF Phase B pilot, with commercial length horizontal wellpairs, was instrumented with two different types of extensometers. While the data from those wells remains confidential, some data exist in the public domain<sup>22</sup>.

**Figure 12** shows the vertical strains approximately 2 years after steaming commenced. Well BE2 is between wellpairs, i.e., ~35m away. Without any temperature change at this location, measurable vertical strains were recorded within the cold oilsands over this 7-month period. The pay zone between 140m and 162m has increased in thickness, and this has resulted in a comparable surface heave.

These data confirm that the oilsands are dilating ahead of the thermal front, in areas unaffected by temperature. The measured increased volume is entirely due to an increase in porosity. This increased porosity must be occupied by water, thereby dramatically increasing the pore fluid mobility. Gas exsolution is not occurring since pressures are increasing, not decreasing, and there is no temperature change here. The total vertical displacement of the top of the reservoir continued upwards through the overburden, with little attenuation.

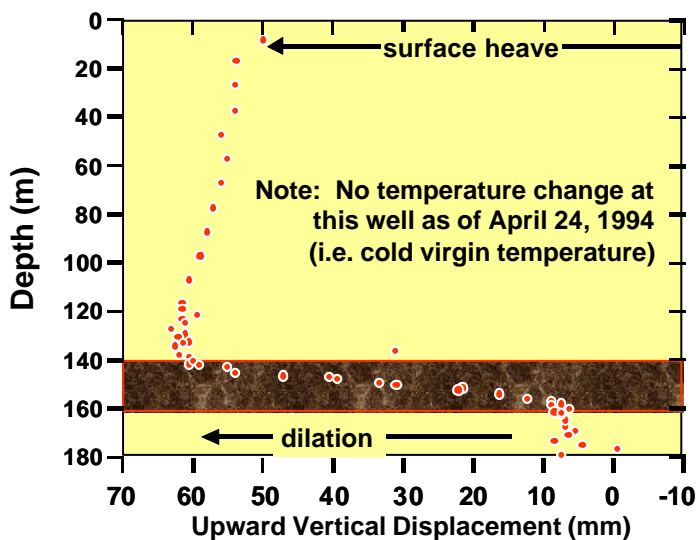


**Figure 12** BE2 extensometer from Sept -93 to Apr-94 (7 months), UTF Phase B  
ref. O'Rourke, Chambers, Suggett & Good (1994)

### Surface Heave

The dilation and shear displacements within the reservoir are seen at surface as displacements and rotations. Short-term events, such as hydraulic fractures, are sometimes monitored with tiltmeters installed within shallow wells drilled from surface. For longer-term monitoring, surface heave data can be used.

In general, the maximum surface heave will be approximately 2% of the reservoir's gross pay thickness. That maximum heave can be expected to taper off to 10% at a distance of twice the project's depth. The surface heaves of deeper projects will taper more gradually away from the nominal pattern perimeter.

**Heave Magnitude** is not normally a concern because everything is raised uniformly. Problems can arise when one area rises relative to another area. Examples include heave under a shoreline or containment pond.

**Slope** can affect systems with gravity flow. Gravity pipelines, and surface drainage (e.g.: ditches, creeks) will have altered hydraulics if the surface heave imposes differential elevations. However, it must be remembered that these differential heaves will occur over years, therefore surface drainage may naturally adapt to any changes in hydraulic profile.

Vertical structures such as power transmission towers, facility stacks, and level-sensitive equipment may less forgiving of becoming out of vertical.

**Curvature** results when there are changes in slope. Curvature has the potential for affecting large linear structures such as long buildings and pipelines by imposing bending stresses. Curvature is probably too small to be problematic, particularly for deeper SAGD projects.

### Monitoring with Satellite Radar Interferometry.

"InSAR" can be used to measure surface heaves, as an alternative to precision ground surveys of a network of survey monuments. Many steam injection pilots have included some survey monuments as part of their instrumentation, however most were too sparse to use for any engineering analyses. Furthermore, extrapolation to any commercial scale project would result in a prohibitive cost both to install the monument array and for periodic surveys.

InSAR measures surface contours at two different time periods, and takes the differential as the surface heave. Because there is a certain degree of imprecision in taking surface measurements of forest and muskeg, an enhanced monitoring system would include highly reflective coherent hard targets with which to calibrate the fuzzy surface readings.

InSAR has been successfully used in the oilpatch for measuring the surface displacements above compacting diatomite reservoirs (Belridge, CA)<sup>23</sup>, and cyclic steam stimulation (Cold Lake<sup>24</sup>, Peace River<sup>25</sup>), amongst others.

**Inversion of Surface Heaves** provides reservoir engineers with the location of sub-surface volume changes, and possibly shear displacements if the data quality is high enough<sup>26</sup>. In a process analogous to seismic conversion, the surface heave data are related to the cumulative effect of subsurface strains. Areas of the reservoir that are swept can be identified to better control the SAGD process and future drilling.

Identifying potential shear zones within and above the reservoir will assist in predicting or detecting casing-formation interaction problems.

### Caprock Integrity

The two requirements to ensure caprock integrity are that there is an adequate hydraulic seal, and that the seal remains mechanically intact. The hydraulic seal must be areally continuous, and have a low vertical transmissibility ( $k_v \cdot h$ ) to ensure that reservoir fluids are contained over the life of the project.

This caprock must have adequate strength and deformation properties to withstand the pressures, temperatures, and deformations imposed by the SAGD process. Key issues to be considered when assessing caprock integrity are:

1. depth of burial
2. shale thickness and strength
3. pay thickness
4. injection pressure
5. steam chamber dimensions

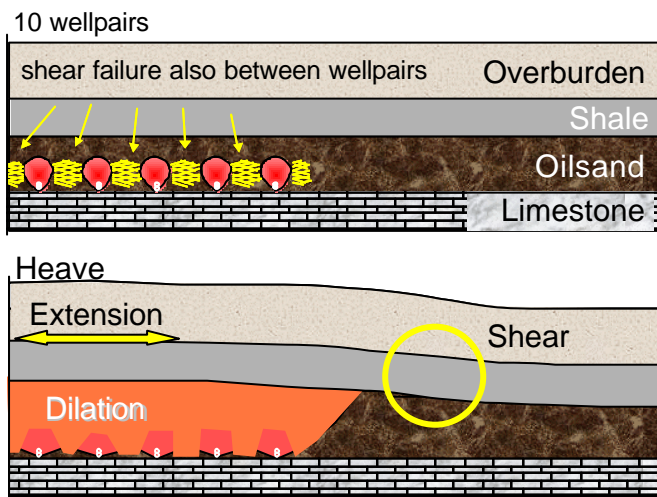


Figure 13 Shear, dilation, and heave associated with SAGD

Figure 13 shows a schematic of a SAGD pattern of 10 wellpairs. As the pattern matures, the diluted oilsand reservoir displaces the overburden, resulting in surface heave. Pressures and temperatures (not shown) are elevated in and around the steam chamber. As a result, the caprock is more severely stressed. The critical stress within the shale caprock may be outside the nominal pattern, as indicated by the circle in the lower diagram.

### CONCLUSIONS

If steam injection pressures are sufficiently high to cause shear failure in the oilsands, the resultant shear dilation significantly enhances the reservoir's porosity, absolute permeability, and relative permeability to water. These beneficial changes are permanent and irreversible. Geomechanics can enhance the SAGD process.

In order to obtain these benefits, the injection pressure must be within 500 kPa of the fracture pressure. Since the limiting fracture pressure is at the top of the steam chamber,

the steam injection pressure must be reduced as the steam chamber rises.

Convective heat flux ahead of the steam chamber was shown to contribute to formation heating, and more importantly, was indicative of shearing of the cold oilsands. Geomechanical shearing contributes to the accelerated growth of the steam chamber. This growth was shown to be directional and was a function of the *in situ* stress state.

Examples of reservoir deformations were discussed in. These subsurface deformations were shown to result in surface heaves, which could affect surface activities and facilities. At the same time, inversion of these surface heaves can provide the location of the subsurface deformations, thereby providing reservoir engineers with a tool to monitor the long-term performance of the SAGD process.

### Nomenclature

CHOPS	= cold heavy oil production with sand
$h$	= thickness
$k_a$	= absolute permeability
$(k_a)_{init}$	= initial absolute permeability
$k_h$	= horizontal permeability
$k_v$	= vertical permeability
$P_{inj}$	= injection pressure
$p$	= pressure
$p_f$	= formation fluid pressure
SAGD	= steam-assisted gravity drainage
$T$	= temperature
TC	= thermo couple
$z$	= vertical depth (metres)

$\phi$  = porosity

$\phi^\circ$  = friction angle

$\sigma_{Hmax}$  = maximum horizontal stress

~ = "approximately"

≡ = "exactly equal to"

### References

- 1) Dusseault, M.B. (1980) "Sample disturbance in Athabasca oil sand", *JCPT*, April-June, pp.85-92.
- 2) Touhidi-Baghini, A. (1998) **Absolute permeability of McMurray Formation oil sands at low confining stresses**, Ph.D. thesis, Dept. of Civil Eng., U. of Alberta, Edmonton, Alberta 339 pp.
- 3) Touhidi-Baghini, A. and J.D. Scott (1998) "Absolute permeability changes of oil sand during shear", *proc. 51<sup>st</sup> Can. Geotechnical Conf.*, Edmonton, Alberta, pp.729-736.
- 4) Butler, R.M. (1997) **Thermal recovery of oil and bitumen**, publ. GravDrain Inc. (2nd printing), Calgary, Alberta, 528pp..
- 5) Dusseault, M. B. and H. R. van Domselaar (1982) "Unconsolidated Sand Sampling in Canadian and Venezuelan Waters", *Proc. Second Int. Conf. on Heavy Crudes and Tar Sands*, UNITAR, Caracas, February 7-17, pp. 165-174.
- 6) Collins, P.M. (2002) "The False Lucre of Low-Pressure SAGD", paper 2004-031, *proc. CIPC*, Calgary, Alberta, Canada, June 8 – 10, 12pp.
- 7) Oldakowski, K. (1994) **Stress induced permeability changes of Athabasca oilsands**, M.Sc. thesis, Dept. of Civil Eng., U. of Alberta, Edmonton, Alberta 227 pp.
- 8) Chalaturnyk, R. and Li, P. (2001) "When is it important to consider geomechanics in SAGD operations?", paper 2001-46,

- proc. Pet. Soc. Of CIM Can. Int. Pet. Conf., June 12-14, Calgary, Alberta.
- 9) Wong, R.C.K. (2004) "Effect of Sample Disturbance Induced by Gas Exsolution on Geotechnical and Hydraulic Properties Measurements in Oil Sands", paper CIPC2004-071, Petroleum Society of CIM, CIPC, Calgary, Alberta, Canada, June 8 – 10, 13pp
  - 10) Aherne, A. and G. Birrell (2002) "Observations relating to non-condensable gasses in a vapour chamber: Phase B of the Dover Project", paper SPE79023/PS2002-519, R2R2R joint CIM/SPE/CHOA conference, Calgary, Alberta, Nov. 4-7, 7pp.
  - 11) Birrell, G. (2001) "Heat transfer ahead of a SAGD steam chamber: a study of thermocouple data from Phase B of the Underground Test Facility (Dover Project)", paper 2001-88, Pet. Soc. of CIM's Can. Int. Pet. Conf., June 12-14, Calgary, Alberta.
  - 12) Ito, Y., M. Ichikawa, and T. Hirata (2000) The growth of the steam chamber during the early period of the UTF Phase B and Hangingstone Phase I projects, paper 2000-05, PS of CIM, Can. Int. Pet. Conf., June 4-8, Calgary, Alberta, 16pp.
  - 13) Collins, P.M. (2002) "Injection pressures for geomechanical enhancement of recovery processes in the Athabasca oil sands", paper SPE/PS-CIM/CHOA 79028, proc. SPE International Thermal Operations and Heavy Oil Symposium and International Horizontal Well Technology Conference, Calgary, Alberta, Canada, 4–7 November, 13pp.
  - 14) Bachu, S. and J.R. Underschultz (1993) "Hydrogeology of Formation Waters, Northeastern Alberta Basin", *AAPG Bulletin* V77 N10, pp. 1745-1768.
  - 15) Chalaturnyk, R.J. (1996) **Geomechanics of the steam assisted gravity drainage process in heavy oil reservoirs**, Ph.D. thesis, Dept. of Civil Eng., U. of Alberta, Edmonton, Alberta 576 pp.
  - 16) Gould, Bryan (2002) presentation on Multilateral CSS for Shell Canada, during "Panel Session 3: Emerging technologies in heavy oil and horizontals", R2R2R joint CIM/SPE/CHOA conference, Calgary, Alberta, Nov. 4-7 (unpublished)
  - 17) Cox, J.W. (1983) "Long axis orientation in elongated boreholes and its correlation with rock stress data";, proc. SPWLA Twenty-Fourth Ann. Logging Symp., June 27-30, 17pp.
  - 18) Dusseault, M. B. (1980) "The behaviour of hydraulically induced fractures in oil sands", **Underground Rock Engineering**, CIM Special Volume 22, pp. 36-41
  - 19) Chhina, H.S., R.W. Luhnig, R.A. Bilak, D.A. Best (1987) "A horizontal fracture test in the Athabasca Oil Sands" pre-print 87-38-56, proc. 38th ATM of the PS of CIM, Calgary June 8-10, 36pp.
  - 20) Ito, Y. and Suzuki, S. (1996) "Numerical Simulation of the SAGD Process in the Hangingstone Oil Sands Reservoir", paper 96-57, proc. 47th ATM of the Petroleum Society of CIM, Calgary, Alberta June 10-12, 14 pp.
  - 21) Collins, P.M (1994) Design of the Monitoring Program for AOSTRA's Underground Test Facility, Phase B Pilot, JCPT, March, V33 N3, pp. 46-53.
  - 22) O'Rourke, J.C., Chambers, J.L., Suggett, J.C., Good, W.K. (1994) "UTF Project Status and Commercial Potential – An Update, May 1994", paper 94-40, proc. 48th ATM of the Pet. Soc. of CIM and AOSTRA, June 12-15, Calgary, Alberta, 24pp.
  - 23) Eaton, S. (2002) "4-D from the heavens: satellite-borne time-lapse radar measures production-induced ground movement", *Nickle's New Technology Magazine*, Sept., pp.5-7.
  - 24) Stancliffe, R.P.W., and M.W.A. van der Kooij, (2001) "The use of satellite-based radar interferometry to monitor production activity at the Cold Lake heavy oil field, Alberta, Canada", *AAPG Bulletin*, V85 N5 pp. 781–793
  - 25) Roche, P. (2005) "Listening to the reservoir: Shell uses microseismic, time-lapse seismic and surface tiltmeters to monitor steam movements at Peace River", *Nickle's New Technology Magazine*, Jan/Feb, V11 N1, pp.28-30.
  - 26) Dusseault MB, and L. Rothenburg (2002). "Deformation analysis for reservoir management", *Oil & Gas Science and Technology - Revue de l'IFP*, V57, N5, pp 539-554

**Metric Conversion Factors**

1 ft = 0.3048 metre  
1 psi = 6.8947 kPa  
1 psi/ft = 22.62 kPa/m  
°F = (°C\*1.8)+32  
1 cP ≡ mPa·s  
1 Darcy = 0.986923 μm<sup>2</sup>

V20050829.2200